SUPPLEMENTAL FIGURE 1

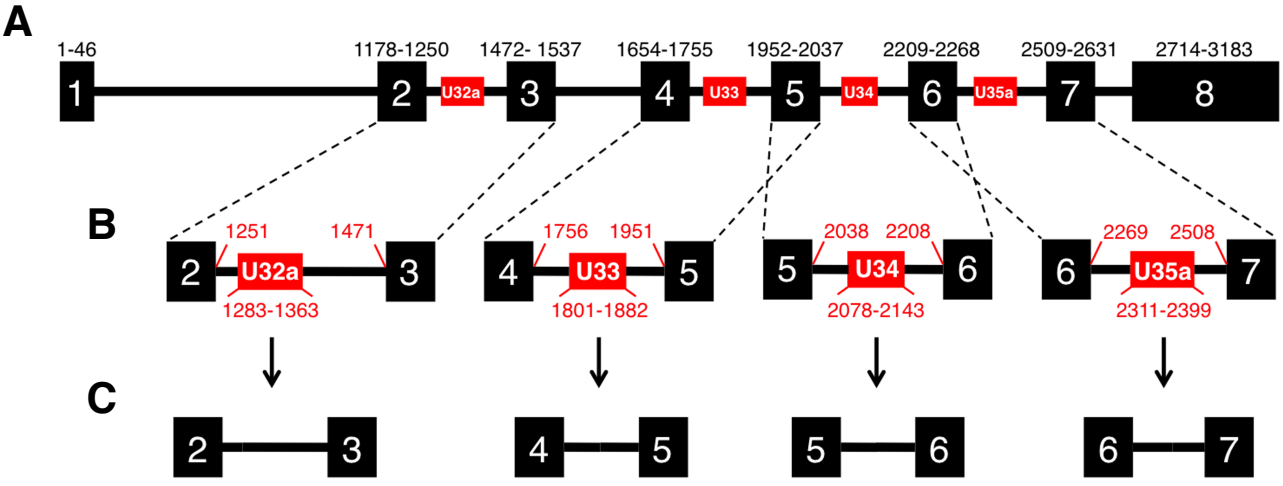

Supplemental Figure 1. Approach for removal of snoRNAs from *Rpl13a* gene.
(A) Wild type *Rpl13a* exon-intron structure is shown, with exons in black and intronic snoRNAs in red rectangles. Numbering in black reflects the limits of the exonic sequences, relative to the translation start of the gene.
(B) Enlarged detail of snoRNA-containing introns is displayed. Numbering in red reflects the limits of the intronic sequences and the snoRNAs, relative to the translation start of the gene.
(C) Targeting construct was generated by removing nucleotides 1283-1363 encoding U32a, nucleotides 1801-1882 encoding U33, nucleotides 2078-2143 encoding U34, and nucleotides 2311-2399 encoding U35a.

SUPPLEMENTAL FIGURE 2

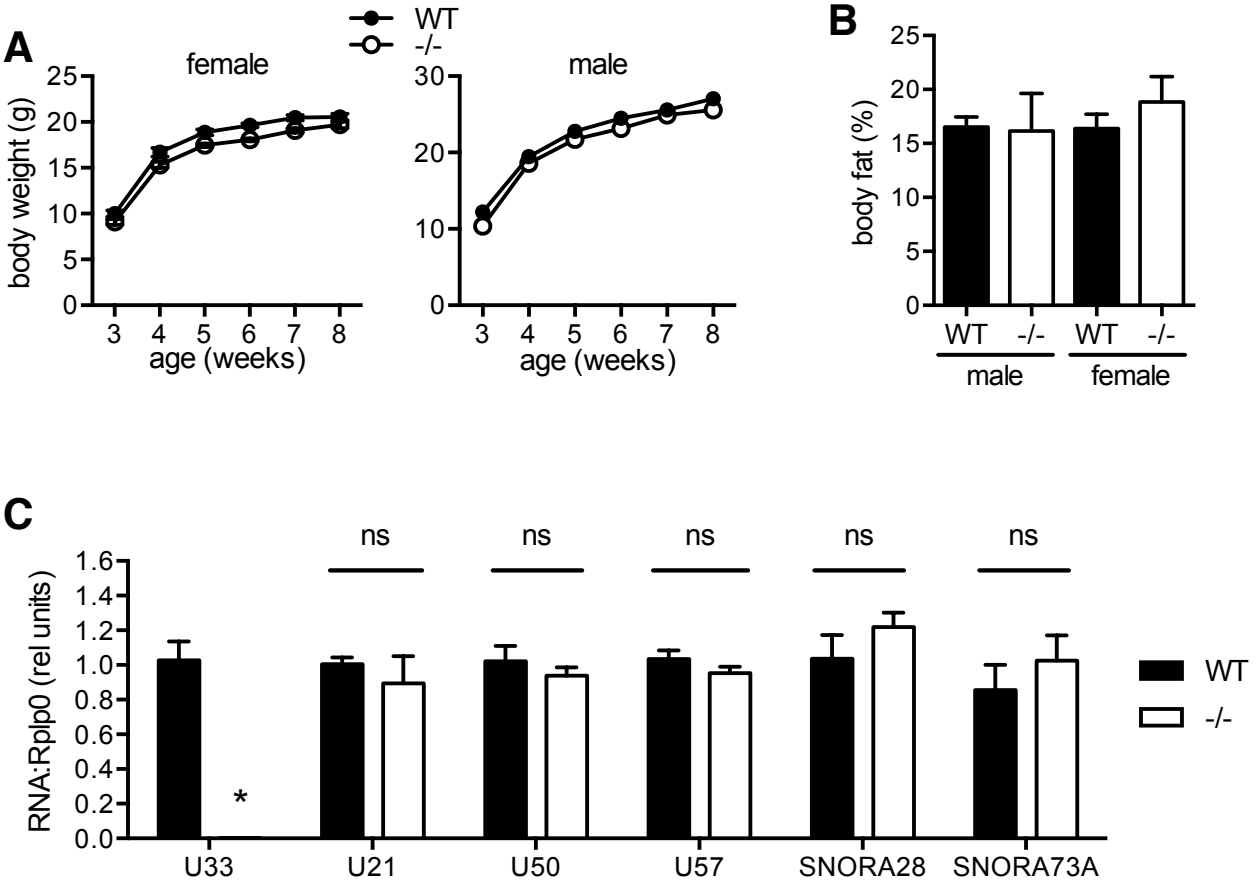

Supplemental Figure 2. Body weight and composition of *Rpl13a*-snoless mice.
(A) Mean (±SE) serial weights for WT (filled circles) and -/- (open circles) mice. n = 10-12 mice/genotype/sex.
(B) Mean percent body fat (+SE) for WT (filled bars) and -/- (open bars) mice at 7 to 8 weeks of age. n ≥ 4 mice/genotype/sex.
(C) qPCR quantified expression (relative to *Rplp0*) of *Rpl13a* snoRNA U33 and 5 unrelated snoRNAs in WT and -/- liver tissue. Mean + standard error (SE) for a minimum of n = 5 mice/genotype.
*, P < 0.001 for -/- vs. WT; ns, non-significant determined by unpaired t-test

SUPPLEMENTAL FIGURE 3

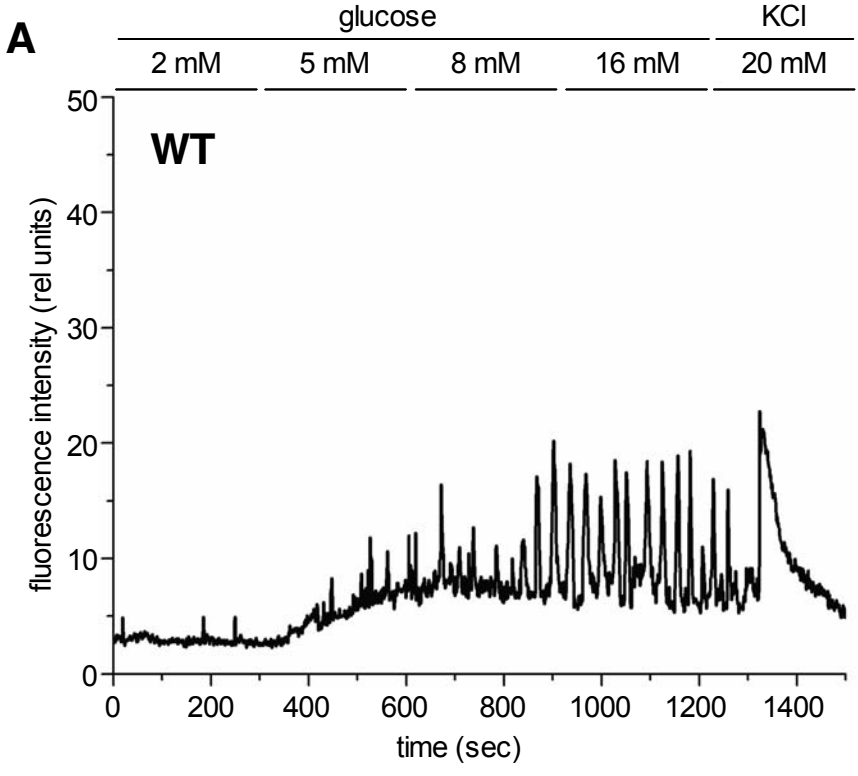

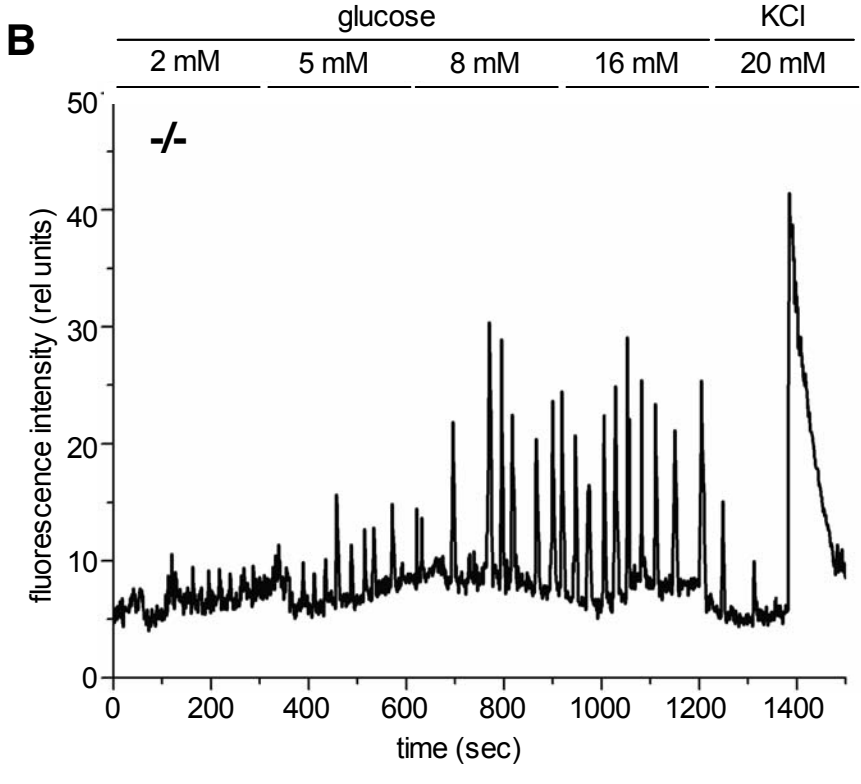

Supplemental Figure 3. Representative calcium oscillations.
Traces of calcium oscillations at 2, 5, 8 and 16 mM glucose, or with addition of 20 mM KCl in representative single β-cell within whole islet from WT (**A**) and -/- (**B**) mouse. As expected, higher glucose concentrations trigger larger calcium oscillations in islets of both genotypes, and addition of KCl triggers fast and maximal influx of calcium into the cytoplasm, resulting in greater spike and consequent decay of fluorescence intensity. Note higher relative change in fluorescence intensity in -/- vs. WT.

SUPPLEMENTAL FIGURE 4

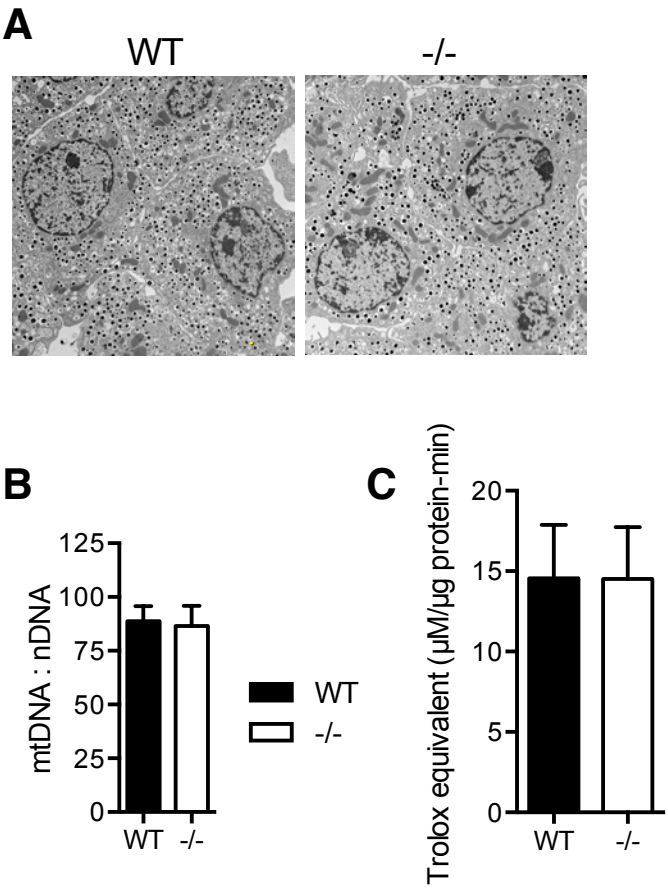

Supplemental Figure 4. Mitochondrial morphology and anti-oxidant capacity are unchanged in *Rpl13a*-snoless islets.
(A) Representative thin section electron micrographs of isolated WT and -/- islets. Scale bar, 2 µm.
(B) Quantification of WT (filled bars) and -/- (open bars) islet mitochondrial DNA (mtDNA) relative to nuclear DNA (nDNA). Means (+SE) for n = 4 mice/genotype.
(C) Trolox equivalent anti-oxidant capacity of lysates from WT and -/- islets for n = 4 mice/genotype

SUPPLEMENTAL FIGURE 5

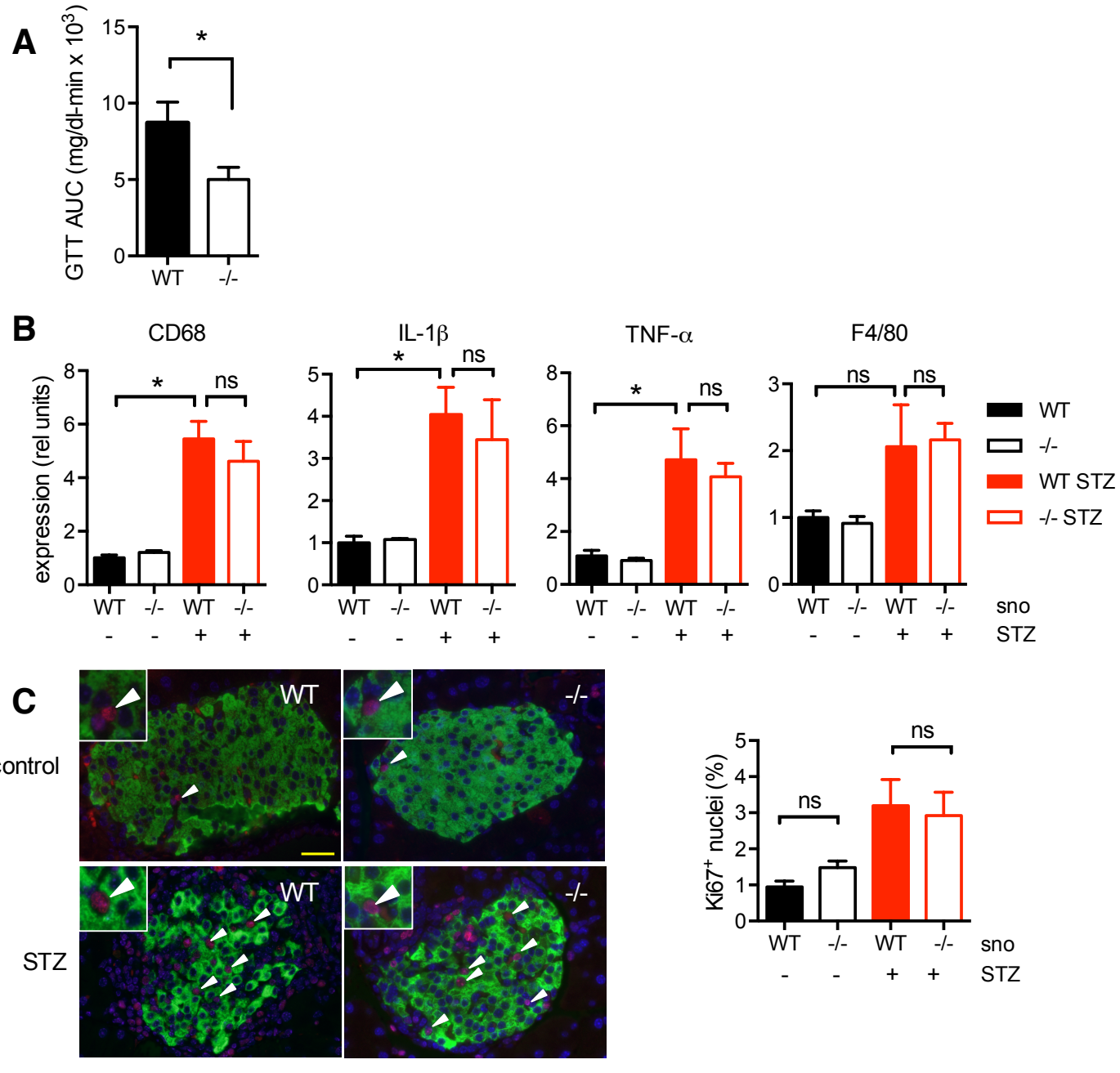

Supplemental Figure 5. STZ-induced inflammation and β-cell replication is indistinguishable between WT and *Rpl13a*-snoless islets.

(A) AUC during GTT in 16-week old WT and -/- mice. n = 9 mice/genotype.

(B) qPCR quantified expression of inflammatory markers (relative to *Rplp0*) in wild type (filled bars) and -/- (open bars) islets 5 days after PBS (black) or STZ (red) treatment. Means (+SE) for n = 3 mice per genotype/treatment.

(C) Representative pancreas sections stained for Ki-67 5 days after STZ. Scale bar, 25 μm. Graph shows quantification of means (+SE) for n = 4 mice per genotype/treatment.

*, $p < 0.05$ for comparisons indicated; ns, not significant determined by unpaired t-test

Supplemental Table 1. Quality Control for RNAseq Samples

Sample	Total reads	Total aligned	% Aligned	% Uniquely aligned	Average length	FRET (average quality)	%GC
Rpl13a-snoless1	43,134,384	34,580,071	70.13%	60.16%	49.93	35.61	51.87%
Rpl13a-snoless2	50,052,151	43,147,485	76.50%	66.87%	49.93	35.76	49.47%
Rpl13a-snoless3	59,238,549	47,915,432	70.90%	61.02%	49.93	35.63	50.78%
Rpl13a-snoless4	55,209,748	45,935,704	73.91%	64.69%	49.92	35.74	49.86%
WT1	76,608,177	61,733,952	70.66%	60.85%	49.93	35.59	51.63%
WT2	53,914,668	46,342,409	77.09%	68.30%	49.93	35.65	51.27%
WT3	57,690,914	47,486,694	73.17%	64.12%	49.94	35.58	52.32%
WT4	59,756,051	50,511,204	74.88%	65.33%	49.94	35.57	52.15%

Supplemental Table 2. Differentially expressed genes between *Rpl13a*-snoless and WT islets

Gene ID	Gene name	Fold change (-/- vs. WT)	P-value	FDR step up	LSMean(-/-)	LSMean(WT)
Arhgef26	Rho guanine nucleotide exchange factor 26	3.15	2.77E-05	4.27E-02	7.65	2.43
Itih4	Inter-alpha-trypsin inhibitor heavy chain H4	19.91	9.02E-06	2.28E-02	16.59	0.83
Mir6240	MiR-6240	2.40	1.45E-05	2.60E-02	62.74	26.13
Rgs2	Regulator of G-protein signaling 2	3.86	4.70E-07	4.25E-03	61.90	16.02
Slc14a2	Urea transporter 2	-3.37	9.73E-06	2.28E-02	2.41	8.10
Upp2	Uridine phosphorylase 2	15.58	7.88E-07	4.25E-03	8.61	0.55

Supplemental Table 3. Primer Sequences; related to Experimental Procedures

PCR for Genotyping	**sequence 5' to 3'**
forward (F)	GAC AGG TTG CTG CTC AGG AAG TAA ATG G
reverse (R)	CCA GAC CTG CTT TCA GAC TTT AGC CTG
qRT-PCR for mRNAs	
Rplp0 F	ATC CCT GAC GCA CCG CCG TGA
Rplp0 R	TGC ATC TGC TTG GAG CCC ACG TT
Rpl13a F	TGA GGT CGG GTG GAA ATA CC
*Rpl13*a R	GGC CTT TTC CTT GCG TTT CT
Ucp2 F	ACA AGA CCA TTG CAC GAG AG
Ucp2 R	GGT TGG CTT TCA GGA GAG TAT C
qRT-PCR for snoRNAs	
universal stem loop reverse primer	TCC CGA CCA CCA CAG CC
U32a F	GAG TCC ATG ATC AGC AAC ACT CAC C
U32a SLRT	GCG TGG TCC CGA CCA CCA CAG CCG CCA CGA CCA CGC CGA GTC TC
U33 F	AGC TTG TGA TGA GAC ATC TCC CAC T
U33 SLRT	GCG TGG TCC CGA CCA CCA CAG CCG CCA CGA CCA CGC ACA GCC TC
U34 F	CGT CTG TGA TGT TCT GCT ATT ACC TAC ATT GTT
U34 SLRT	GCG TGG TCC CGA CCA CCA CAG CCG CCA CGA CCA CGC AGC GTC TC
U35a F	CTC ACG ATG GTC TTC GGA TG
U35a SLRT	GCG TGG TCC CGA CCA CCA CAG CCG CCA CGA CCA CGC TCC TGG CA
U21 F	GCC AAT GAT GAC ACC ACA CTA ACT GA
U21 SLRT	GCG TGG TCC CGA CCA CCA CAG CCG C
U50 F	TCT ATG ATG ATC CTA TCC CGA AC
U50 SLRT	GCG TGG TCC CGA CCA CCA CAG CCG C
U57 F	GAT GAA CGA ACT TGG CCT GAC CTT C
U57 SLRT	GCG TGG TCC CGA CCA CCA CAG CCG C
SNORA73A F	AAC GGG AGC TTA GGG CAT T
SNORA73A SLRT	GCG TGG TCC CGA CCA CCA CAG CCG CCA CGA CCA CGC TTT TGT
SNORA28 F	CCG TCT GAC ACA ATT TGA GC
SNORA28 SLRT	GCG TGG TCC CGA CCA CCA CAG CCG CCA CGA CCA CGC TTT GTT AG